AIP | Journal of Applied Physics

Sub-ambient carbon dioxide adsorption properties of nitrogen doped graphene

P. Tamilarasan and Sundara Ramaprabhu

Citation: Journal of Applied Physics **117**, 144301 (2015); doi: 10.1063/1.4917205
View online: http://dx.doi.org/10.1063/1.4917205
View Table of Contents: http://scitation.aip.org/content/aip/journal/jap/117/14?ver=pdfcov
Published by the AIP Publishing

JOURNAL OF APPLIED PHYSICS **117**, 144301 (2015)

Sub-ambient carbon dioxide adsorption properties of nitrogen doped graphene

P. Tamilarasan and Sundara Ramaprabhu[a)]
Alternative Energy and Nanotechnology Laboratory (AENL), Nano Functional Materials Technology Centre (NFMTC), Department of Physics, Indian Institute of Technology Madras, Chennai 600036, India

(Received 31 January 2015; accepted 28 March 2015; published online 8 April 2015)

Carbon dioxide adsorption on carbon surface can be enhanced by doping the surface with heterogeneous atoms, which can increase local surface affinity. This study presents the carbon dioxide adsorption properties of nitrogen doped graphene at low pressures (<100 kPa). Graphene was exposed to nitrogen plasma, which dopes nitrogen atoms into carbon hexagonal lattice, mainly in pyridinic and pyrrolic forms. It is found that nitrogen doping significantly improves the CO_2 adsorption capacity at all temperatures, due to the enrichment of local Lewis basic sites. In general, isotherm and thermodynamic parameters suggest that doped nitrogen sites have nearly same adsorption energy of surface defects and residual functional groups. The isosteric heat of adsorption remains in physisorption range, which falls with surface coverage, suggesting the distribution of magnitude of adsorption energy. The absolute values of isosteric heat and entropy of adsorption are slightly increased upon nitrogen doping. © *2015 AIP Publishing LLC*.
[http://dx.doi.org/10.1063/1.4917205]

I. INTRODUCTION

The sharp acceleration in CO_2 emissions due to industrial revolution leads to imbalance in our ecosystem and results in global warming. In this regards, solid state adsorbents for carbon dioxide storage attain importance in environmental perspectives.[1] Storage options are economically feasible, since the adsorbed gas can be utilized for industrial needs. An adsorbent must possess high surface area, denser adsorption sites, and good regenerability. Zeolites, metal chalcogenide nanostructures, organometallics, polymers, activated carbon, and graphitic carbon nanomaterials are widely studied solid state CO_2 adsorbents.[2–4] Particularly, graphene showed high adsorption capacity compared to other graphitic nanostructures, due to its high surface area and planar structure associated with the two-dimensional crystal structure formed by sp^2 hybridized carbon.[5] Generally, exfoliated few layered graphene sheets are highly wrinkled, which results in spacious interlayer and highly accessible surface area that facilitates CO_2 storage at the interlayer space.[6]

In general, selective functionalization improves the performance of the materials. In CO_2 adsorption, non-covalent functionalities, such as metal/metal chalcogenide nanoparticles and polymers, are widely employed functionalities.[7,8] On the other hand, covalent functionalities, such as organic groups and doped heterogeneous atoms, also perform better.[9] The influence of surface covalent functional groups on CO_2 adsorption properties has been extensively documented.[10] Heterogeneous atoms significantly alter the electronic properties of host lattice and change the local surface reactivity.[11] Particularly, nitrogen atoms are well recognized dopant in electron density enhancement for electrochemical device applications, where doped nitrogen injects electron density into the graphitic carbon lattice.[12] Nitrogen doping localizes the HOMO and LUMO levels of graphitic materials, which can be viewed as localized Lewis basic sites with good affinity towards Lewis acidic species, such as CO_2 molecules.[13,14] Here, nitrogen atoms create net positive charge on adjacent carbon atoms within carbon framework due to the electron-accepting ability.[15] Moreover, doping nitrogen into the carbon hexagonal lattice is comfortable, due to the similar atomic size and the valency of nitrogen that mimics sp^2 hybridized carbon atom, which results in stable $C_{1-x}N_x$ configuration.

Nitrogen doped activated carbon,[16] carbon monoliths,[17] carbon nanotubes,[15] and carbon aerogels[18] have been reported as adsorbents for carbon dioxide. Fu *et al*. have studied the CO_2 adsorption on nitrogen-doped porous aromatic frameworks.[19] Kemp *et al*. have determined the CO_2 adsorption on nitrogen doped graphene (N-HEG) produced by chemical activation of graphene oxide/polyaniline composite.[16] The results suggest importance of N content, apart from pore size and surface area, in achieving optimal CO_2 adsorption in graphitic materials with good selectivity.[16] However, the thermodynamic aspects of CO_2 adsorption in nitrogen doped graphene are yet to be investigated. Similar materials have been synthesized by chemical activation of graphene/polyindole and graphene/polypyrrole composites and determined their CO_2 adsorption capacity.[20,21] Here, functionalization followed by chemical activation helped to achieve CO_2 adsorption capacities as high as those of activated high surface area carbon.

Besides, it is essential to understand the isothermal and thermodynamic parameters of interaction between the heteroatom doped surface and adsorbate molecules in order to develop new class of high performance adsorbents. In this study, we have studied the low pressure CO_2 adsorption

a)Email: ramp@iitm.ac.in

isotherm and thermodynamic properties of nitrogen doped graphene, where nitrogen atoms were doped by exposing graphene to nitrogen plasma. To the best of our knowledge, this is the first experimental attempt to understand the thermodynamic aspects of CO_2 adsorption on nitrogen doped graphene at low pressures.

II. EXPERIMENTAL SECTION

A. Nitrogen doped graphene synthesis

Graphene has been synthesized from graphite by a two step top-down process. In the first step, pure graphite was oxidized to graphite oxide (GO) by Hummers' method using a water-free mixture of concentrated sulphuric acid, hydrogen peroxide, sodium nitrate, and potassium permanganate.[22] In the second step, GO was heated at 473 K under hydrogen atmosphere in a tubular furnace, which results in exfoliation of few layered reduced graphene, denoted as hydrogen exfoliated graphene (HEG).[23] The specific surface area of HEG has been calculated in our previous study using BET equation and found to be 344 $m^2\ g^{-1}$, while the specific pore volume was 1.94 $cm^3\ g^{-1}$.[23] Further, 50 mg of HEG was exposed to nitrogen plasma (13.56 MHz, 130 W) for 30 min at 10 kPa chamber pressure using a RF Magnetron sputtering system and labeled as N-HEG.[24] We assume that physical surface area will not be significantly changed upon nitrogen doping. The structural and molecular vibrational characteristics of N-HEG have been reported in our recent study.[25]

B. Characterization techniques

The morphology of HEG and N-HEG was recorded by high-resolution transmission electron microscopy (Technai G-20). The X-ray photoelectron spectrum of N-HEG is recorded by SPECS X-ray photoelectron spectrometer equipped with Mg Kα (1253 eV) X-ray source and PHOIBOS 100MCD energy analyzer at ultrahigh vacuum (10^{-8} Pa). Low pressure carbon dioxide adsorption-desorption studies were carried out using a surface area analyzer (Micromeritics ASAP 2020), which is capable of operating up to 100 kPa pressure.

C. Analysis procedure

The adsorption-desorption properties of N-HEG were determined by vacuum-swing adsorption technique, where the adsorbate was degassed at reduced pressure. Approximately 200 mg of N-HEG was loaded to a sample cell of known mass (m_1), where the sample cell consists of a sample tube, a seal frit (20 μm pore size), and a filling rod. The sample was degassed and activated at 373 K for 3 h under reduced pressure (~7 Pa) and measured the total mass of the cell with sample (m_2). The difference $m_2 - m_1$ gives sample mass with ±0.001 mg accuracy. The free space (available volume inside the sample cell) was calculated using high pure helium gas at respective analysis temperatures. The sample temperature was maintained by a thermally insulated water bath and an isothermal jacket.

In a typical adsorption isotherm analysis, known amount (n) of demoisturized high pure CO_2 gas was allowed into the sample cell. At equilibrium, the unabsorbed gas (n_{eq}) inside the tube has been calculated from the available volume, equilibrium pressure, and sample temperature, using van der Waals equation,

$$\left(P_{eq} + \frac{n^2 a}{V^2}\right)(V - n_{eq} b) = n_{eq} RT, \tag{1}$$

where P_{eq} is the equilibrium pressure of n_{eq} moles of CO_2 gas at temperature T in volume V.[26] Hence, adsorbed amount, n_{ad}, is equal to the difference $n - n_{eq}$ at equilibrium, i.e., $n_{ad} = n - n_{eq}$.

Similarly, in desorption analysis, known amount of gas (n^*) has been removed from the total amount of gas inside the tube ($n = n_{ad} + n_{eq}$). Hence, the total amount of gas (sum of adsorbed and free molecules) is $n - n^*$. Once again the amount of unabsorbed gas (n_{eq}^*) at equilibrium desorption pressure in the known volume (V) was determined by Eq. (1). The amount of CO_2 molecules reside on the surface of adsorbent, n_{ad}^*, is equal to $n - n^* - n_{eq}^*$ at equilibrium. The interaction of CO_2 molecules with adsorbent has been determined by adsorption isotherm analysis. Henry's constant gives the affinity of the surface towards adsorbate assuming no influence from the adsorbed molecules on approaching molecule at very low adsorbed amount, which is represented as,

$$k_H = \lim_{x \to 0} \frac{P}{x}, \tag{2}$$

where k_H is the Henry's constant, x is the amount of gas adsorbed (gram per gram of adsorbent), and P is the CO_2 pressure. Since the number of anchoring sites per unit mass of sample is not available, here Henry's constant has been described as the pressure required to store CO_2 molecules equal to the mass of adsorbent.

At low pressures (around 100 kPa), the adsorption can be modeled by Langmuir and Freundlich adsorption isotherm models assuming each adsorption site holds only one adsorbate molecule. Langmuir model assumes that all adsorption sites have equal energy, while Freundlich model considers the possible distribution of adsorption energies.

Langmuir isotherm[27] is represented as,

$$Q_{eq} = \frac{Q_{\max} K_L P}{1 + K_L P}, \tag{3}$$

while Freundlich equation[28] is,

$$Q_{eq} = K_F P^{\frac{1}{n}}, \tag{4}$$

where Q_{eq} (mol g^{-1}) is the amount of adsorbed CO_2 molecules at equilibrium pressure P (Pa), Q_{max} (mol g^{-1}) is the maximum adsorption capacity at complete monolayer coverage, K_L is Langmuir isotherm coefficient, K_F is Freundlich isotherm constant (mol g^{-1}), and n is adsorption intensity.

Enthalpy and entropy change of adsorption were obtained from adsorption isosteres (van't Hoff plot) at multiple constant adsorbed amounts. The slope of the adsorption isosteres gives differential enthalpy of adsorption according to Clausius-Clapeyron equation,

$$\Delta H = R\left(\frac{\partial \ln P}{\partial(1/T)}\right)_n, \quad (5)$$

where P is the pressure and T is the temperature. The absolute value of ΔH gives the "isosteric heat" of adsorption ($|\Delta H|$). The intercept ($\Delta S/R$) of extrapolated isosteres with $ln\ P$-axis in van't Hoff plot gives change in entropies (ΔS) associated with adsorption.[29]

III. RESULTS AND DISCUSSIONS

A. Morphological analysis

TEM images of HEG (Figure 1(a)) display the highly disordered wrinkled structure of few layer graphene, where the wrinkles occur due to the rapid removal of intercalated functional groups in the presence of hydrogen.[23] In addition, it has to be noted that the edges of the graphene sheets are folded in order to minimize dangling bonds.[30] The wrinkles (groove like structure) are produced by introducing structural defects (pentagons and heptagons) into the hexagonal lattice, which also can function as anchoring sites for CO_2 molecules. It is reported that CO_2 molecules find grooves as suitable sites for accommodation.[31] Figure 1(b), TEM image of N-HEG, shows no damage in graphene layers upon exposure to nitrogen plasma. Here, it is expected that 75% to 90% of nitrogen atoms are doped by simple substitution of surface carbon atoms in the graphene lattice, which results in significantly unaffected lattice structure.[32] The rest of the doped nitrogen (10%–25%) may be attached to the dangling bonds at the edges and surface defects. The formation energy of "nitrogen doping" is much lesser than that of "nitrogen + vacancy" formation.[33] Hence, the system is prone to simply substitute carbon by nitrogen atom or to attach nitrogen with unsaturated bonds.

B. Elemental analysis of N-HEG

The survey spectrum (Fig. 2(a)) shows the presence of nitrogen along with carbon and oxygen. The strong signal corresponding to oxygen can be imputed to the presence of residual oxygen containing functional groups. The nitrogen concentration is around 3.9 wt. % determined from the survey spectrum.

The high-resolution N1s spectrum, shown in Figure 2(b), has been deconvoluted into three distinct peaks centered at 398.9, 400.2, and 401.6 eV with equal full width half maxima. The peaks located at about 398.9 and 400.2 eV, respectively, correspond to pyridinic (39.1%) and pyrrolic (44.1%) nitrogen. The peak at 401.6 eV from quaternary nitrogen (16.8%) arises, while carbon atoms are substituted by nitrogen atoms within the graphene network and are known as "graphitic" nitrogen. It is reported that reactivity of pristine and N-doped graphene has the following trend: pristine graphene < graphitic N-G < pyrrolic N-G < pyridinic N-G.[13] In the synthesized material, pyridinic and pyrrolic type contributes about 83% of the total doped nitrogen, which results in high affinity towards CO_2 molecules. These nitrogen atoms inject a pair of electrons into the π-conjugated system and alter the HOMO and LUMO distribution in graphene.

The deconvoluted high-resolution C1s spectrum (Figure 2(c)) has five distinct peaks at 284.9, 286.1, 287.4, 289.2, and 290.3 eV.[34] The major feature of this deconvoluted spectrum is located at 284.9 eV corresponding to graphitic or sp^2-hybridized carbon. The nitrogen atoms present in graphene network with C-N and C=N configurations result peaks at 286.1 and 287.4 eV, respectively. Here, C=N configuration may result from the nitrogen doping into the sp^3 hybridized carbon network produced by wrinkles. It is well known that the curvature in sp^2 hybridization admixes a small amount of sp^3 bonding.[35] Integration of these peaks reveals that almost 27% of nitrogen is doped in sp^3 hybridized carbon network. This may be attributed to the presence of large amount of wrinkles on the surface of graphene. The features of carboxyl groups are found at ~289.2 eV. The low intense peak at 290.3 eV can be imputed to the $\pi - \pi^*$ satellite, which is commonly found in the hexagonal arrangement of carbon atoms.

C. Adsorption isotherm analysis

The adsorption isotherms were obtained for N-HEG up to 100 kPa equilibrium pressure at multiple temperatures (Fig. 3). The equilibrium specific adsorption capacity (Q_{eq}) has been reported by normalizing the adsorbed amount (n_{ad} or n_{ad}*) to the absolute mass of sample (m).

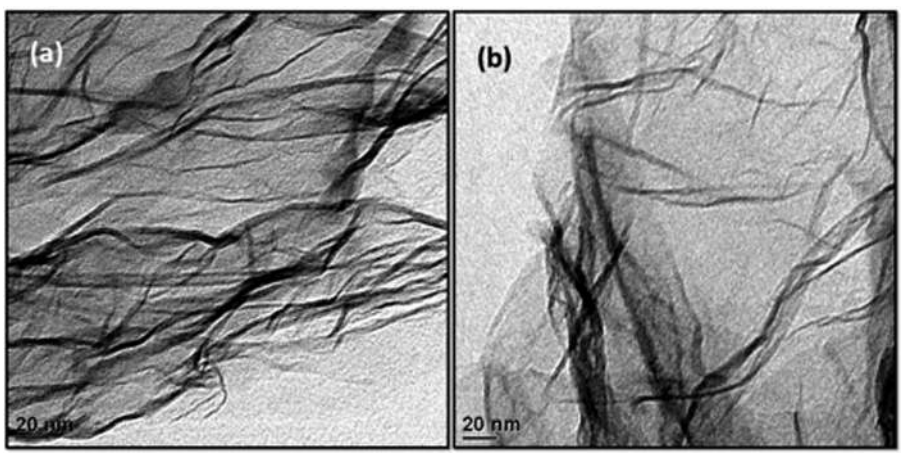

FIG. 1. TEM images of (a) HEG and (b) N-HEG.

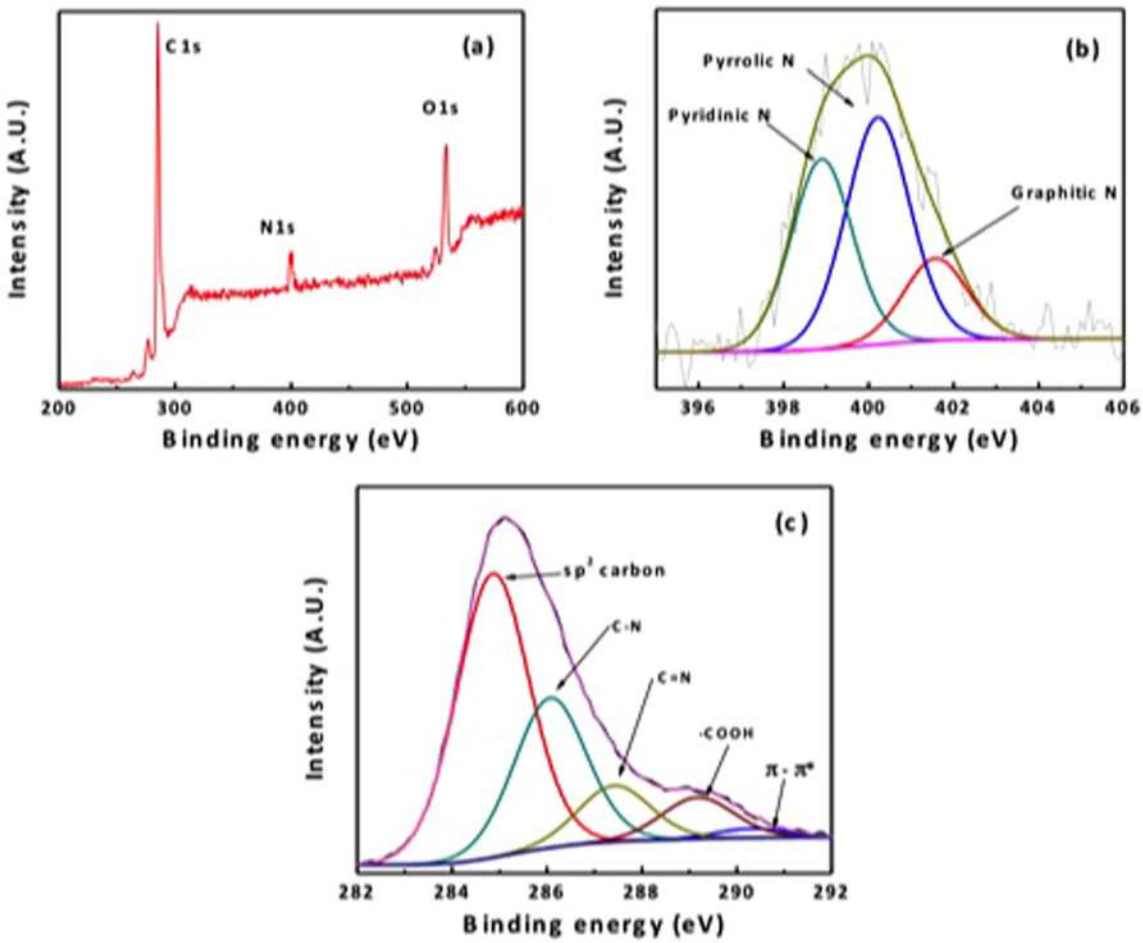

FIG. 2. XPS spectrum of N-HEG. (a) Survey scans normalized to C1s, (b) high-resolution N1s, and (c) high-resolution C1s spectrum.

Adsorption isotherms of N-HEG show that the equilibrium adsorption capacity is 742 μmol g^{-1} at 283 K with ~100 kPa CO_2 gas pressure, while that of HEG was found to be 695 μmol g^{-1} at similar conditions.[36] In addition, adsorption isotherms of N-HEG closely follow those of HEG. This enhancement can be imputed to the presence of doped nitrogen atoms. Nitrogen doping alters local electronic structure of graphene, which can act as anchoring sites for CO_2 molecules. Equilibrium adsorption capacity decreases with increase in temperature due to thermally driven high kinetic energy of CO_2 molecules.

Henry's constants (k_H) are calculated by fitting the experimental data up to <10 kPa equilibrium pressure, since isotherms are not linear at the whole range. In addition, we obtained the k_H values for HEG as well using isotherms from our previous study.[36] Table I shows that the value of

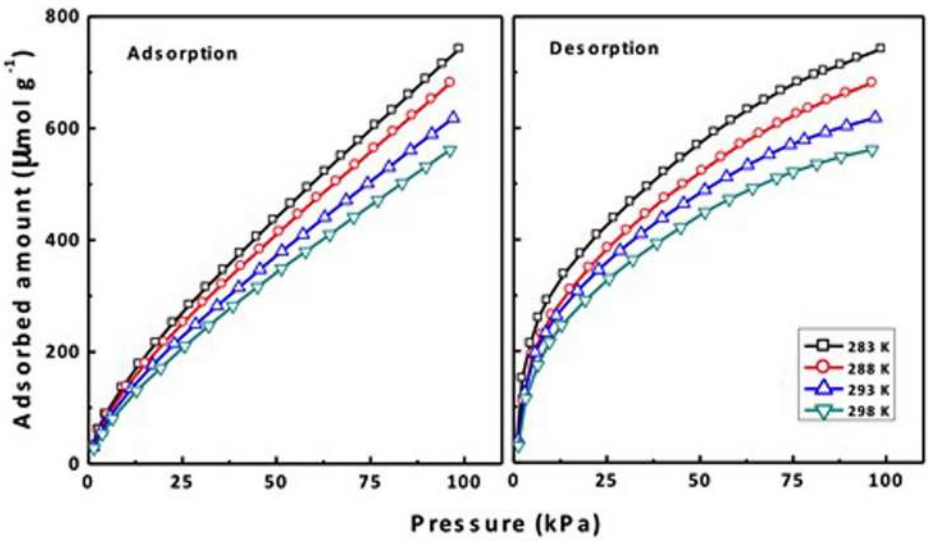

FIG. 3. CO_2 adsorption-desorption isotherms of N-HEG at different sample temperatures.

TABLE I. Comparison of adsorption isotherm parameters of HEG and N-HEG. Units: Q_{eq} (μmol/g), Q_{max} (μmol/g), K_L (k Pa^{-1}), n (A.U.), and K_F (μmol g^{-1} k Pa$^{-(1/n)}$).

				Langmuir			Freundlich			
Material	T (K)	Q_{eq} at 100 kPa	k_H (bar)	Q_{max}	K_L	R^2	n	K_F	K_F/n	R^2
HEG[a]	283	695	13.32	1390	0.0095	0.941	1.47	30.93	21.04	0.999
	288	609	15.96	1241	0.0094	0.992	1.47	27.64	18.80	0.999
	293	558	18.55	1171	0.0089	0.993	1.44	23.64	16.41	0.999
	298	512	22.25	1098	0.0082	0.995	1.42	20.05	14.12	0.999
N-HEG	283	742	12.50	1791	0.0097	0.983	1.5	32.76	21.83	0.999
	288	681	14.70	1662	0.0094	0.990	1.49	30.15	20.26	0.999
	293	618	16.78	1503	0.0092	0.993	1.48	27.39	18.50	0.999
	298	561	19.51	1368	0.0089	0.995	1.48	24.68	16.75	0.999

[a]From our previous study.[36]

Henry's constant of CO_2 adsorption on HEG is slightly decreased upon nitrogen doping. Here, doped nitrogen atoms interact with CO_2 molecules and increase the bulk affinity of adsorbate. In general, k_H values increase with temperature due to the fact that CO_2 molecules get high kinetic energy and escapes from the adsorption site at high temperatures.

In general, adsorption isotherms of HEG and N-HEG fit better with Freundlich model compared with Langmuir model, which suggests the distribution of adsorption energy. However, Langmuir model did not deviate largely, which may be attributed to the narrow adsorption energy distribution. In HEG, structural defects and residual functional groups are the major anchoring sites. Upon nitrogen doping, surface is enriched with adsorption sites, which leads to higher adsorption capacity. But, R^2 values indicate that doped nitrogen sites also has adsorption energy close to those of structural defects and residual functional groups. Substantially, Henry's constant also evoke that nitrogen sites compete with native adsorption sites with nearly same adsorption energy.

The saturation adsorption capacity (Q_{max}) of N-HEG is significantly (300–400 μmol g^{-1}) higher than that of HEG and decreases with increase in temperature. It is also observed from K_L values that the initial adsorption rate is increased upon nitrogen doping and decreased with temperature. Moreover, the decrease in K_L and Q_{max} values with temperature indicates that there is no competing temperature assisted chemical reaction between CO_2 and nitrogen sites.[37]

Freundlich coefficient, n, values indicate the favorability of adsorption, which suggests the favorable adsorption of CO_2 on N-HEG. Here, nitrogen sites should be imputed to the improvement.[37] It is also reported a linear relationship between the experimentally determined Freundlich coefficient (n) and HOMO density, which suggests that nitrogen doping increases the HOMO density and thus the adsorptivity. Another Freundlich parameter, K_F, is related to the total molecular orbital energy of adsorbate and adsorbent system. The value of K_F/n gives the information about the adsorption energy, which displays that the adsorption energy is also slightly increased as the nitrogen sites provide significant contribution. This is in good agreement with the literature.[13]

Conclusively, nitrogen doping increases favorability and adsorption energy, which leads to a significant improvement in adsorption capacity. Wu *et al*. have studied the reactivity of nitrogen doped graphene, which shows that the reactivity depends on the type of doped nitrogen.[13] Here, the spatial distribution of HOMO and LUMO levels of α and β electrons in pristine graphene was found to be delocalized. But nitrogen doping localizes the HOMO and LUMO distributions of α and β electrons, since nitrogen doping introduces an unpaired electron. It is also reported that electron density of both adsorbate and adsorbent is one of the major factors determining the adsorption properties.[38] This causes the localized distribution of the molecular orbital and enhances the affinity of graphene with foreign molecules.

This can be explained with distribution of electrostatic potential (EP, the net electrical field of the electrons and nuclei) as well, where pristine graphene shows uniform distribution of EP on defect-free surface. But it is more positive at the edges due to the unsaturated bonds, which has slightly higher reactivity (or adsorptivity). Surface defects and residual functional groups also can alter the adsorptivity. Thus, the pristine graphene has fewer adsorption sites, which results in the low adsorptivity. Nevertheless, distribution of EP changes significantly upon nitrogen doping, where positive EP regions have been produced on the doped nitrogen sites. These sites offer additional adsorption sites for CO_2 molecules and increase adsorption capacity. Furthermore, the magnitude of positive EP is higher for pyridinic, followed by pyrrolic and graphitic nitrogen sites, respectively, which may reflect directly on the adsorptivity.

Generally, desorption isotherms do not follow the same lend of adsorption due to the porous nature and affinity of adsorbent surface, which leads to a hysteresis. In our previous study, we defined a quantity, called *isothermal adsorbate retention (IAR)*, in order to analyze the desorption behavior. This is defined as the amount of CO_2 retained on adsorbate when isothermally desorbed at the same pressure.

Mathematically,

$$IAR = Q_{eq}(des) - Q_{eq}(ads), \tag{6}$$

where $Q_{eq}(ads)$ and $Q_{qe}(des)$ are the equilibrium adsorbate concentration at certain pressure on adsorption and corresponding desorption isotherms, respectively.

The *IAR* behavior of N-HEG (Figure 4) shows that the adsorbent retains 157, 145, 132, and 120 μmol g^{-1} at 50 kPa

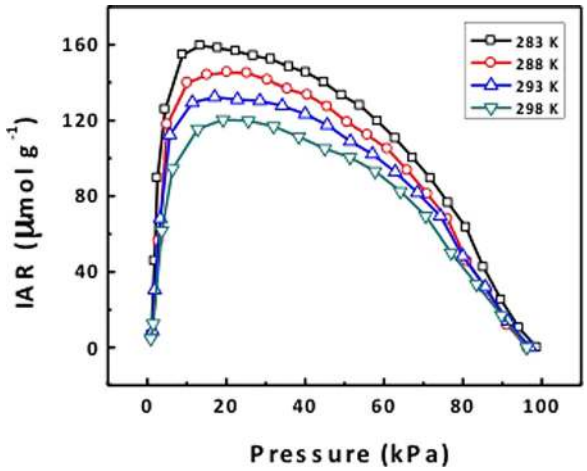

FIG. 4. Isothermal adsorbate retention of N-HEG as a function of equilibrium pressure.

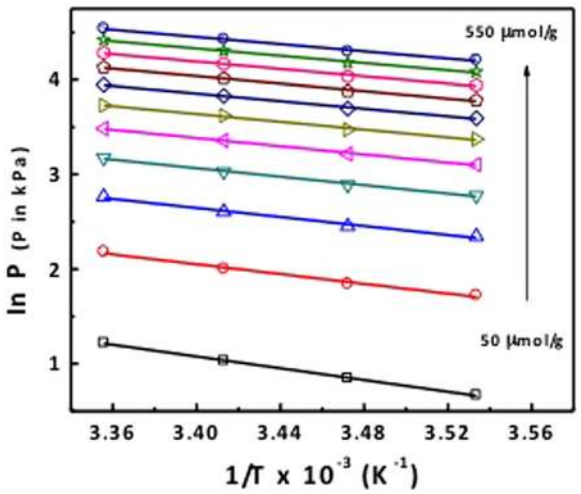

FIG. 5. CO_2 adsorption isosteres (van't Hoff plot) of N-HEG with different adsorbed amount.

desorption pressure and 283, 288, 293, and 298 K, while those of HEG was 56, 54, 51, and 46 μmol g^{-1} at same conditions, respectively. It also has to be noted that the increase in *IAR* value is even higher than the enhancement in adsorption capacity. This suggests that doped nitrogen sites may have slightly higher adsorption energy than that of structural defects and residual functional groups, which is in agreement with the obtained adsorption energy. Although the retention is increased upon nitrogen doping, the CO_2 molecules are desorbed till $\sim$5 μmol g^{-1} residue at very low pressure ($\sim$1 kPa), suggesting good recoverability of the adsorbent similar to those observed in HEG.

The intersection of extrapolated straight line fit of *IAR*-raise and *IAR*-fall regions gives the onset pressure of IAR drop at low pressure. The approximate values of onset pressure of *IAR* have been calculated to be 5.6, 7.1, 8.2, and 8.9 kPa at 283, 288, 293, and 298 K sample temperature, respectively. The increase in onset pressure with temperature can be attributed to the temperature assisted desorption.

D. Thermodynamics of adsorption

The regression lines of *ln* (*pressure*) vs. *1/T* at constant adsorbed amount (50–550 μmol g^{-1}) are the adsorption isosteres of N-HEG (van't Hoff plot), presented in Figure 5. The isosteres closely follow Arrhenius relation suggesting the temperature-dependency of adsorption, while negative slope indicates that the adsorption is exothermic, i.e., physisorption, which decreases with increasing temperature.

The strength of interaction between adsorbate and adsorbent has been represented by the isosteric heat of adsorption ($|\Delta H|$), which is the absolute value of differential enthalpy. This can be viewed as the difference between activation energies for adsorption and desorption. The $|\Delta H|$ values are calculated from the slope of adsorption isosteres at multiple adsorbed amounts, using Clausius-Clapeyron equation (Eq. (5)).

Figure 6 displays the isosteric heat of CO_2 adsorption on N-HEG as a function of adsorbed amount. The N-HEG surface shows continuous variations in values of isosteric heat of adsorption with surface coverage, suggesting the heterogeneity of the surface, resulted by the doped nitrogen and residual functional groups.[39]

Moreover, it has to be noted that the change in $|\Delta H|$ value with surface coverage follows similar trend of HEG, since there is no chemically interacting molecules included into the structure. As it can be assumed that the gas density on adsorbent surface with pressure has ideal dependence at low pressures (<100 kPa), the gradual fall in $|\Delta H|$ value has to be attributed to the continuously distributed adsorption energy of heterogeneous adsorbent surface. Briefly, adsorption takes place only due to the interaction between the adsorption site and CO_2 molecule. The priority of adsorption exclusively depends on the adsorption energy of the site. Hence, initially approaching molecules will be attached with relatively higher binding energy, while the excess molecules are loosely adhered with low energy. This leads to the lower adsorption energy for the excess molecules, which may loosely adhere with the adsorbent. The doped nitrogen occurs in three different forms (pyridinic, pyrrolic, and graphitic) with different strength of interaction. Moreover, surface defects and residual functional groups also contribute to adsorption with different energy. This leads to a dispersion

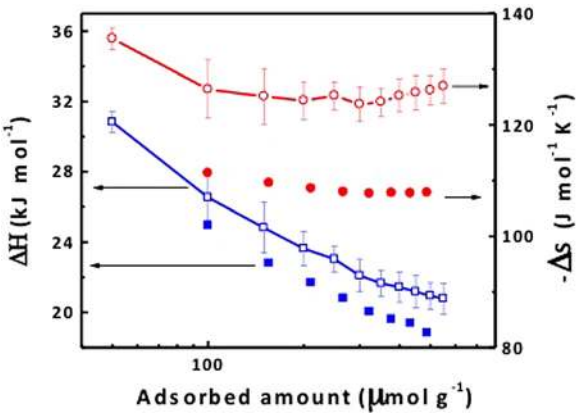

FIG. 6. Isosteric heats and entropy change in adsorption of CO_2 on N-HEG (open symbol) and HEG (solid symbol) as a function of adsorbed amount. Data corresponding to HEG have been adopted from our previous report.[36]

of adsorption energy. In general, the $|\Delta H|$ values of N-HEG are slightly higher than that obtained for the pristine HEG, due to the presence of nitrogen sites. This is in good agreement with the conclusion derived from K_F/n values and with the literature.[15] Hence, we can deduce that adsorption of CO_2 molecule on an N-HEG is energetically favorable than that on a pristine HEG.

The entropy change in adsorption of CO_2 ($-\Delta S$) was calculated from the intercepts of adsorption isosteres with *ln P*-axis ($\Delta S/R$) in van't Hoff plot at corresponding adsorbed amount. The pattern of entropy change upon surface coverage has also been presented in Figure 6, which indicates that ΔS value of CO_2 adsorption on N-HEG with surface coverage follows the similar trend of HEG. The surfaces of both HEG and N-HEG are heterogeneous, where the heterogeneity is introduced by structural defects (wrinkles and edges), residual functional groups in HEG, and additionally nitrogen atoms in N-HEG. Hence, the entropy of a system does not change significantly at higher surface coverage ($>100\,\mu$mol g^{-1}). It has to be noted that the value of entropy is decreased with surface coverage in both cases due to the fact that entropy of adsorbed gas molecule tends towards that of bulk gas.[40] This indicates the conventional behavior of physisorption on heterogeneous surface.

Figure 6 clearly shows that the ΔS values of CO_2 adsorption on N-HEG are significantly increased compared to pristine HEG adsorbent. Nitrogen doping localizes the HOMO and LUMO distributions of α and β electrons as it injects unpaired electrons. Further, the adsorption properties strongly depend on the electron densities of both adsorbates and adsorbents.[38] As discussed in isotherm analysis, interaction of CO_2 molecules is slightly stronger with nitrogen sites compared with surface adsorption sites of HEG, i.e., localized charge distribution is strongly disturbed and increases the disorder in the system. We believe that this might be the major reason for the increase in the ΔS values of CO_2 adsorption on N-HEG. Typically, CO_2 adsorption on HEG and N-HEG has the ΔS values of -111 and $-135\,J\,mol^{-1}\,K^{-1}$ at $100\,\mu$mol g^{-1} surface coverage, respectively.

IV. CONCLUSION

In this study, we have doped nitrogen atoms into graphene lattice using nitrogen plasma, where around 83% of nitrogen atoms accommodate pyridinic and pyrrolic sites in the carbon hexagonal lattice. Low pressure CO_2 adsorption-desorption isothermal properties of N-HEG have been experimentally determined at multiple temperatures. Nitrogen doping increases CO_2 adsorption capacity of graphene. Although the *IAR* values have been increased upon nitrogen doping, the residual adsorbed CO_2 at low pressures ($\sim$1 kPa) reaches as low as $5\,\mu$mol g^{-1} residue. The values of Henry's constant suggest that nitrogen doping increases the affinity of adsorbate. Simulated adsorption isotherms suggest that nitrogen sites compete with the residual functional groups and structural defects with slightly higher adsorption energy. Hence, the favorability and adsorption capacity of N-HEG are higher than pristine HEG, due to increased adsorption energy and density of adsorption sites, respectively. The change in adsorption properties has been mainly attributed to the localized HOMO and LUMO distributions of α and β electrons. The values of isosteric heat of CO_2 adsorption on N-HEG are slightly higher than those of pristine HEG. The value of entropy is decreased with surface coverage for both HEG and N-HEG adsorbents suggesting the physical interaction of heterogeneous surface with CO_2 molecules.

ACKNOWLEDGMENTS

The authors acknowledge NFMTC-IITM for XPS and HRTEM analyses. One of the authors (P.T.) acknowledges Indian Institute of Technology Madras (IITM) for the financial supports (senior research fellowship).

[1]J. Pires, F. Martins, M. Alvim-Ferraz, and M. Simões, Chem. Eng. Res. Des. **89**, 1446 (2011).
[2]Q. Wang, J. Luo, Z. Zhong, and A. Borgna, Energy Environ. Sci. **4**, 42 (2011).
[3]P. Tamilarasan and S. Ramaprabhu, Int. J. Greenhouse Gas Control **10**, 486 (2012).
[4]J. D. Baniecki, M. Ishii, K. Kurihara, K. Yamanaka, T. Yano, K. Shinozaki, T. Imada, and Y. Kobayashi, J. Appl. Phys. **106**, 054109 (2009).
[5]A. K. Mishra and S. Ramaprabhu, AIP Adv. **1**, 032152 (2011).
[6]A. Kaniyoor, T. T. Baby, T. Arockiadoss, N. Rajalakshmi, and S. Ramaprabhu, J. Phys. Chem. C **115**, 17660 (2011).
[7]A. K. Mishra and S. Ramaprabhu, J. Appl. Phys. **116**, 064306 (2014).
[8]P. Tamilarasan, T. S. Remya, and S. Ramaprabhu, Graphene **1**, 3 (2013).
[9]P. Tamilarasan and S. Ramaprabhu, J. Appl. Phys. **116**, 124314 (2014).
[10]M. S. Shafeeyan, W. M. A. W. Daud, A. Houshmand, and A. Shamiri, J. Anal. Appl. Pyrol. **89**, 143 (2010).
[11]M. Pumera, J. Mater. Chem. C **2**, 6454 (2014).
[12]P. Lazar, R. Zboril, M. Pumera, and M. Otyepka, Phys. Chem. Chem. Phys. **16**, 14231 (2014).
[13]P. Wu, P. Du, H. Zhang, and C. Cai, Phys. Chem. Chem. Phys. **15**, 6920 (2013).
[14]S. van Dommele, K. P. de Jong, and J. H. Bitter, Chem. Commun. **2006**, 4859.
[15]I. D. Mackie and G. A. DiLabio, Phys. Chem. Chem. Phys. **13**, 2780 (2011).
[16]K. C. Kemp, V. Chandra, M. Saleh, and K. S. Kim, Nanotechnology **24**, 235703 (2013).
[17]G. P. Hao, W. C. Li, D. Qian, and A. H. Lu, Adv. Mater. **22**, 853 (2010).
[18]A. S. Ello, J. A. Yapo, and A. Trokourey, Afr. J. Pure Appl. Chem. **7**, 61 (2013).
[19]J. Fu, J. Wu, R. Custelcean, and D.-e. Jiang, J. Colloid Interface Sci. **438**, 191 (2015).
[20]V. Chandra, S. U. Yu, S. H. Kim, Y. S. Yoon, D. Y. Kim, A. H. Kwon, M. Meyyappan, and K. S. Kim, Chem. Commun. **48**, 735 (2012).
[21]M. Saleh, V. Chandra, K. C. Kemp, and K. S. Kim, Nanotechnology **24**, 255702 (2013).
[22]W. S. Hummers and R. E. Offeman, J. Am. Chem. Soc. **80**, 1339 (1958).
[23]A. Kaniyoor, T. T. Baby, and S. Ramaprabhu, J. Mater. Chem. **20**, 8467 (2010).
[24]V. B. Parambhath, R. Nagar, and S. Ramaprabhu, Langmuir **28**, 7826 (2012).
[25]P. Tamilarasan and S. Ramaprabhu, J. Nanosci. Nanotechnol. **15**, 1154 (2015).
[26]J. D. Van Der Waals, *On the Continuity of the Gaseous and Liquid States* (Courier Dover Publications, 2004).
[27]I. Langmuir, J. Am. Chem. Soc. **38**, 2221 (1916).
[28]H. Freundlich, *Kapillarchemie: eine Darstellung der Chemie der Kolloide und verwandter Gebiete* (Akademische verlagsgesellschaft mbh, 1922).
[29]W. Gao, D. Butler, and D. L. Tomasko, Langmuir **20**, 8083 (2004).
[30]Z. Liu, K. Suenaga, P. J. Harris, and S. Iijima, Phys. Rev. Lett. **102**, 015501 (2009).
[31]M. Bienfait, P. Zeppenfeld, N. Dupont-Pavlovsky, M. Muris, M. R. Johnson, T. Wilson, M. DePies, and O. E. Vilches, Phys. Rev. B **70**, 035410 (2004).

[32]L. Zhao, R. He, K. T. Rim, T. Schiros, K. S. Kim, H. Zhou, C. Gutiérrez, S. P. Chockalingam, C. J. Arguello, L. Pálová, D. Nordlund, M. S. Hybertsen, D. R. Reichman, T. F. Heinz, P. Kim, A. Pinczuk, G. W. Flynn, and A. N. Pasupathy, Science **333**, 999 (2011).
[33]E. Gracia-Espino, U. pez, F. as, H. Terrones, and M. Terrones, Mater. Express **1**, 127 (2011).
[34]H. Nolan, B. Mendoza-Sanchez, N. Ashok Kumar, N. McEvoy, S. O'Brien, V. Nicolosi, and G. S. Duesberg, Phys. Chem. Chem. Phys. **16**, 2280 (2014).
[35]S. Dresselhaus, G. Dresselhaus, and P. Avouris, *Carbon Nanotubes: Synthesis, Structure, Properties, and Applications* (Springer, 2001).
[36]P. Tamilarasan and S. Ramaprabhu, J. Mater. Chem. A **3**, 101 (2015).
[37]Y. Otake, N. Kalili, T. H. Chang, and E. Furuya, Sep. Purif. Technol. **39**, 67 (2004).
[38]E. G. Furuya, H. T. Chang, Y. Miura, and K. E. Noll, Sep. Purif. Technol. **11**, 69 (1997).
[39]S. A. Al-Muhtaseb and J. A. Ritter, J. Phys. Chem. B **103**, 2467 (1999).
[40]C. Pierce and R. N. Smith, J. Phys. Colloid Chem. **54**, 795 (1950).